Pyrrole-stabilized free carbenes generated from alkynyl imidates or aldimines and electrophilic alkynes give pyrrolone- or pyrrole-containing products

Qian Xu, Jingyang Shi and Thomas R. Hoye*

Department of Chemistry, University of Minnesota, 207 Pleasant St. SE, Minneapolis, MN 55455 USA

Abstract

Pyrrole and 2-pyrrolone derivatives are valuable heterocyclic compounds and while classical condensation methods for their synthesis have a long history, many of the recent developments for their preparation involve the use of transition metal catalysis. We report here a complementary, metal-free strategy for constructing structurally diverse derivatives of these heterocycles. The key feature of the approach is the in situ creation of a reactive intermediate by an initial facile event that simultaneously generates a pyrrole ring bearing a free carbene. This is straightforwardly accessed via a spontaneous, net (3+2) cyclization reaction of a linear alkynyl O-silylimidate or alkynyl aldimine with an electrophilic alkyne. The carbene then undergoes either 1,4-silyl migration (to produce 2-pyrrolone derivatives) or C–H insertion, cycloaddition, cyclopropanation, or macrocyclization reactions (leading to pyrrole derivatives).

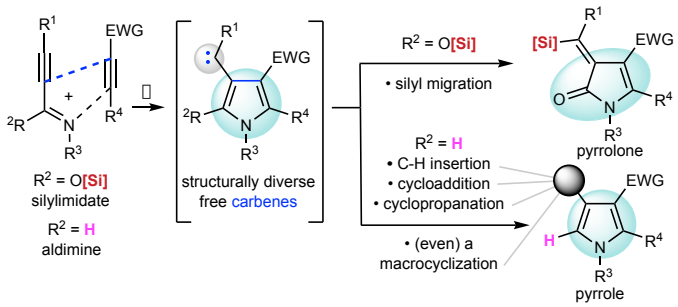

Introduction

Pyrrole (**1**, . 1a) is an essential heterocycle ubiquitous in pharmaceuticals[1,2,3], natural products[4,5], dyes[6], and semiconductors[7]. The drugs sunitinib (**2**) and atorvastatin (**3**) contain a pyrrole core. These respectively show antitumor and antilipidemic bioactivity[2]. Acortatarin A is a secondary metabolite, isolated in 2010 from *Brassica campestris*, a Chinese herbal medicine[8]. It inhibits formation of high-glucose-induced reactive oxygen species (ROSs) in mesangial cells[9]. 3-Methylene-2-pyrrolone (**5**) is a closely related analog of pyrrole; 4E1RCat (**6**) is a pyrrolone derivative that inhibits the eucaryotic initiation factor eIF4E/4G[10].

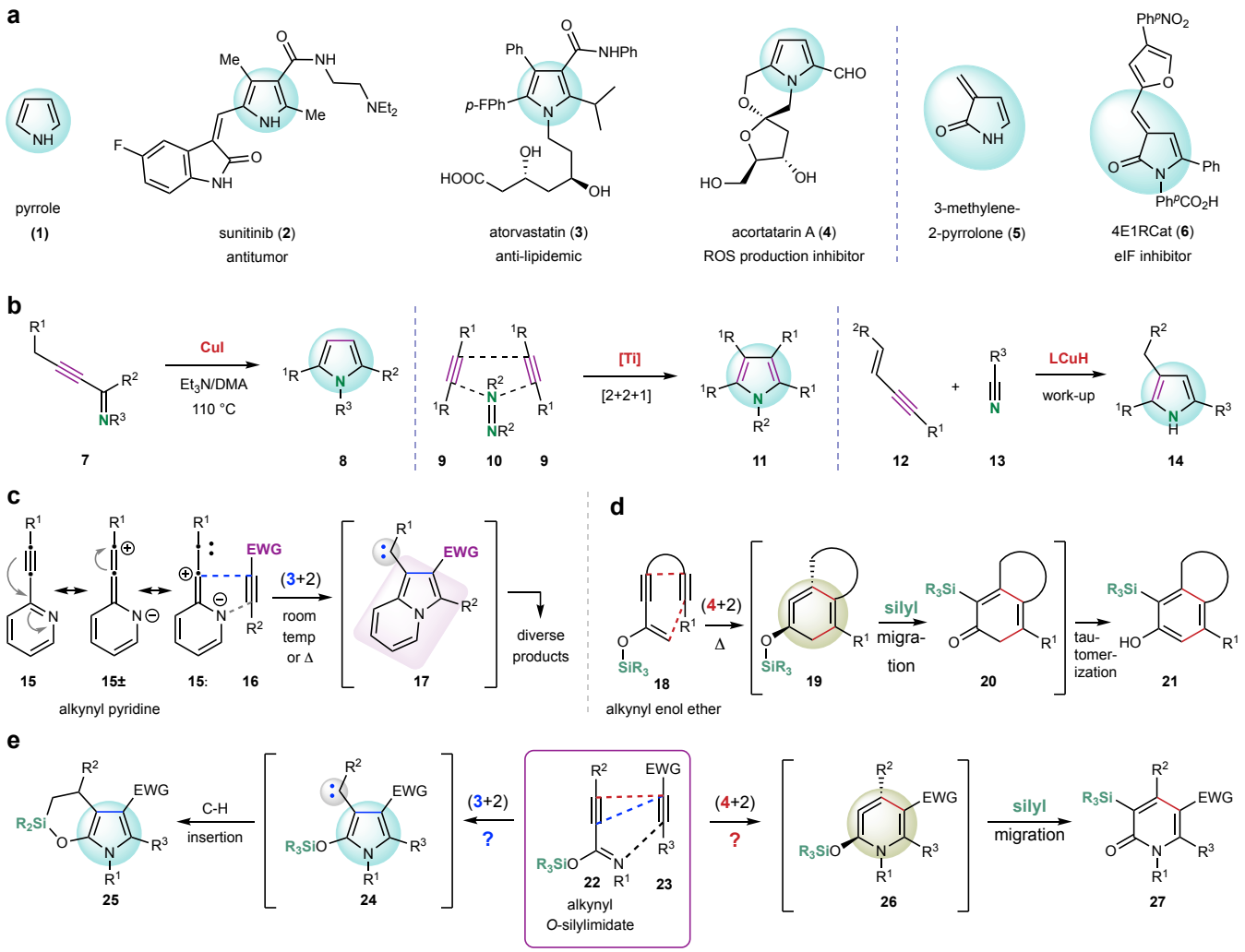

Fig. 1 | Pyrrole is a prized heterocycle. a, Examples of pyrrole- and 2-pyrrolone-containing bioactive molecules. **b**, Examples of modern methods for synthesis of pyrroles using alkyne(s) as a building block(s). **c**. 2-Alkynyl pyridines and electrophilic alkynes fuel the formation of free carbenes conjugated to an indolizine core[17]. **d**, Tetradehydro-Diels-Alder (TDDA) reaction of **18** gives rise to the strained cyclic allene **19**. **e**, This work: two plausible competing cycloaddition pathways [(3+2) vs. (4+2)] for the reaction of **22** with **23** leading to either carbene **24** enroute to pyrrole **25** or aza-cyclic allene **26** enroute to pyridone **27**. DMA = dimethylacetamide; LCuH = liganded copper hydride; EWG = electron-withdrawing group.

Classical methods for pyrrole synthesis are typically based on condensation chemistry between, e.g., carbonyl compounds and amines[11,12,13]. More recently, methods using alkyne-containing substrates for the de novo construction of the pyrrole core have been developed as versatile and complementary strategies (Fig. 1b). For example, the Gevorgyan group reported that alkynyl imines **7** undergo a CuI-catalyzed cycloisomerization reaction to afford a series of mono- and di-substituted pyrroles **8**[14]. Isotope labeling established an allenyl imine tautomer of

7 as the key intermediate. The Tonks group has recently demonstrated a Ti^{II}/Ti^{IV} cycle as an efficient catalytic method to furnish per-substituted pyrroles **11** via a net (2+2+1) cycloaddition reaction from two molecules of alkyne **9** and half of a diimide **10**[15]. In 2020, the Buchwald group discovered that in situ-formed copper hydride can promote the net reductive (3+2) cycloaddition reaction between an enyne **12** and a nitrile **13** to deliver the pyrrole **14** as the product after aqueous work-up[16]. The key intermediate in this process was also proposed as an allenyl imine species. Each of these above-mentioned transformations requires use of a transition metal catalyst and is consummated by the formation of the pyrrole core.

Reactive intermediates (RIs) are short-lived species that have high potential energy and that react with a low kinetic barrier (E_{act}). Because of these virtues, RIs have been extensively studied and have provided considerable fundamental understanding of reactivity that is valuable in the practical construction of new chemical entities. In the realm of carbon-centered RIs, radicals, carbocations, and carbenes are the principal species having fewer than eight valence electrons (i.e., the neon inert gas electronic configuration).

If the construction of a pyrrole moiety could be accompanied by the simultaneous generation of a RI, access to a structurally more diverse array of pyrrole derivatives could emerge from a single synthetic manipulation. As shown in Fig. 1c, our group recently revealed that a 2-alkynyl pyridine (cf. **15**) and an electrophilic alkyne (cf. **16)** could fuel the formation of a free carbene (cf. **17**) merely by mixing and warming both alkyne partners (for one specific set of structures see **29-conf-3** + **30** to zwitterion **31** to **32-conf-1±/32-conf:** in Fig. 2b)[17]. Carbene **17** participated in classical C-H bond insertion and cyclopropanations[18] along with various other transformations leading to structurally diverse indolizine-containing products. Given the significance of pyrrole derivatives, we viewed that access to analogous pyrrole-stabilized carbenes would represent a valuable advance.

The potential for a linear iminoalkyne such as **22** (Fig. 1e) to react with an electrophilic alkyne such as **23** in analogous (3+2) fashion to that of **15** + **16** to carbene **17** was attractive. However, in previous studies, we had observed that silyl enol ethers **18**, carbon analogs of **22**, underwent tetradehydro-Diels-Alder (TDDA) reactions to give the strained cyclic allenes **19** (Fig. 1d)[19]. These underwent a further strain-promoted silyl migration[20] event to deliver the cyclohexadienones **20**, enroute to their phenol tautomers **21**. Therefore, the (4+2) cycloaddition between **22** + **23** is another reasonable pathway that would give rise to the aza-cyclic allene **26** instead of the desired pyrrole **24**. The siloxy group in **22** was selected judiciously to inform us about these two competitive pathways: it could either i) annihilate the carbene **24** via a C-H bond insertion to afford the pyrrole product **25** or ii) undergo a strain-promoted silyl group migration within **26** to furnish the pyridone **27**.

Results and Discussion

In this study, computational and experimental investigations were performed in parallel and proved to be synergistically beneficial. We began by learning the preparation and reactivity of alkynyl imidates **22**. An imine with a siloxy substitution is known as an *O*-silyl imidate; it is typically in equilibrium with its (often) more stable *N*-silyl amide tautomer (cf. **29** vs **28**, Fig. 2a)[21,22]. This mixture of tautomers is often used as a silylating agent for derivatization of *O*-nucleophiles such as those in alcohols and carboxylic acids. Thus, they are also sensitive to moisture. We can only locate a single report of an *O*-silyl-*C*-alkynyl imidate[23]. The rarity of this chemical entity is consistent with our density functional theory (DFT) study (Fig. 2a): namely, the more stable amide tautomer **28** is computed to be 4.9 kcal mol^{-1} (the Boltzmann weighted) lower in Gibbs energy compared to the imidate **29**, indicating that the amide accounts for >99.9% of the equilibrating mixture. Importantly, we identified a unimolecular transition structure (TS) **TS-1** that directly connects **28-conf-1** with **29-conf-1** on the potential energy surface (PES) via a readily surmountable activation barrier (21.8 kcal mol^{-1}, meaning a half-life of 14 min at ambient temperature).

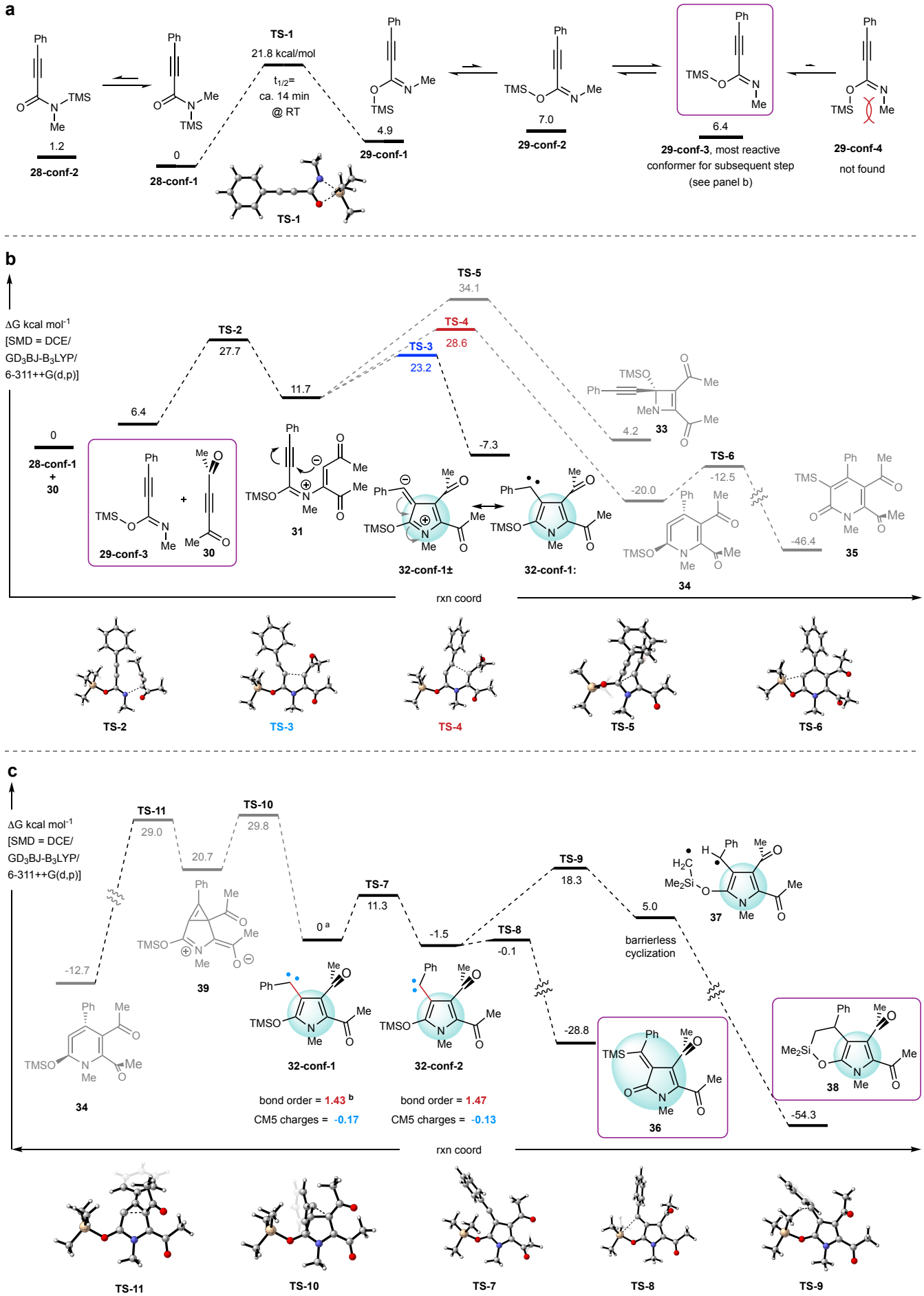
a
TS-1
21.8 kcal/mol
t1/2= ca. 14 min @ RT
1.2
28-conf-2
0
28-conf-1
4.9
29-conf-1
7.0
29-conf-2
6.4
29-conf-3, most reactive conformer for subsequent step (see panel b)
29-conf-4
not found
b
ΔG kcal mol-1
[SMD = DCE/ GD3BJ-B3LYP/ 6-311++G(d,p)]
TS-5
34.1
TS-4
28.6
TS-3
23.2
TS-2
27.7
6.4
11.7
-7.3
0
28-conf-1 + 30
29-conf-3
30
31
32-conf-1±
32-conf-1:
4.2
33
-20.0
TS-6
-12.5
-46.4
35
34
rxn coord
TS-2
TS-3
TS-4
TS-5
TS-6
c
ΔG kcal mol-1
[SMD = DCE/ GD3BJ-B3LYP/ 6-311++G(d,p)]
TS-11
29.0
TS-10
29.8
20.7
-12.7
39
34
0 a
TS-7
11.3
-1.5
TS-8
-0.1
TS-9
18.3
5.0
barrierless cyclization
37
-28.8
36
-54.3
38
32-conf-1
bond order = 1.43 b
CM5 charges = -0.17
32-conf-2
bond order = 1.47
CM5 charges = -0.13
rxn coord
TS-11
TS-10
TS-7
TS-8
TS-9

Fig. 2 | DFT-computed PES for the reaction starting with 28 and 30. a, The amide tautomer **28** interconverts with its less stable imidate isomer **29** via a low-barrier unimolecular process (**TS-1**, 21.8 kcal mol^{-1}). **b**, The (3+2) cycloaddition between **29** and **30** (**TS-3**) is kinetically more favorable than the (4+2) or (2+2) pathways (via **TS-4** or **TS-5**). **c**, 1,4-Silyl migration from the oxygen to the carbon atom in carbene **32-conf-2** is the kinetically most favorable process, while the interconversion of **32-conf-1** to the allene **34** via the cyclopropene **39** has a prohibitively high barrier. TMS = trimethylsilyl; RT = room temperature;

DFT: [SMD (DCE)/B3LYP-GD3BJ/6-311++G(d,p)]. [a] The energies in Fig. 2c are all normalized to 0.0 for **32-conf-1** to more easily discern the relative energy of each stationary state in this panel. [b] Bond orders were obtained using the Wiberg bond index analysis[24].

We next used DFT to study the PES (Fig. 2b) for the reaction between the model trimethylsilyl imidate **29-conf-3** and the diketone **30**, a conformationally simplified electrophilic alkyne analog of dimethyl acetylenedicarboxylate (DMAD). These engage one another with a computed activation barrier of 21.3 kcal mol^{-1} leading to the zwitterionic intermediate **31**. This has three modes for potential cyclization: 4-endo to **33**, 6-endo to **34**, or 5-exo to **32-conf-1**, which is a hybrid of zwitterion (**32-conf-1±)** and carbene (**32-conf-1:)** resonance contributors. A TS for each mode was found and the 5-exo process had the lowest barrier. Although the cyclic allene **34** could have released its strain by a low-barrier silyl migration (cf. **TS-6**) to furnish the pyridone **35**, the barrier for forming **34** (cf. **TS-4)** was computed to be significantly higher leading to the pyrrole carbene **32-conf-1** (cf. **TS-3**). Despite the low equilibrium population of conformer **29-conf-3**, it can still initiate further reaction (Curtin-Hammett principle[25]) because the nitrogen atom in an imidate is expected to be more nucleophilic than the oxygen atom in an amide[26,27,28].

Encouraged by this initial DFT analysis, we first prepared the alkynyl amide **40a** (Fig. 3a) and achieved its silylation using TIPSOTf. The resulting product was highly labile to silica gel, making it challenging to purify. After numerous trials, we settled on pentane as a good solvent for the silylation step because the product is soluble in pentane while the byproduct triethylammonium triflate (Et_3NHOTf) phase-separates. Pentane removal provided the amide of suitable purity for the subsequent reactions. For simplicity, we will describe the product of the silylation step as the reactive imidate tautomer **41a** (and for all other silylated amides as well).

To our delight, the reaction between **41a** and dimethyl acetylenedicarboxylate (DMAD, **42**) cleanly led to a single product as a yellow crystalline material. Distinguishing between the pyridone **43a** and the pyrrolone **44a** as the structure of this product by nuclear magnetic resonance (NMR) spectroscopy was not trivial. We again turned to DFT to examine the energetics of a possible pathway by which the carbene **32** could proceed to the pyridone skeleton (Fig. 2c, left). We located **TS-10** that converted **32-conf-1** to the strained cyclopropene **39**, which could further undergo a ring expansion via **TS-11** to give the cyclic allene **34** enroute to pyridone **35** by a low barrier silyl migration step (via **TS-6**, Fig. 2b). Alternatively, **32-conf-1** was seen to easily isomerize to **32-conf-2** via **TS-7**. The expected C-H insertion reaction within the latter (cf. **24** to **25** in Fig. 1e) was computed to proceed in a stepwise process involving a 1,6-H atom transfer (via **TS-9**) and a subsequent barrierless diradical recombination to deliver the bicyclic pyrrole **38**. However, the fastest process of all was seen as the low barrier silyl migration within **32-conf-2** (via **TS-8**) to deliver the 2-pyrrolone **36**.

To assign the structure of the product obtained from reaction of **41a** with **42**, we first performed NMR computation and then analyzed the data with DP4+[29], which pointed to the pyrrolone **44a** as the more likely structure [see Fig. S1, Supplementary Information (SI)]. Finally, an x-ray diffraction analysis unambiguously confirmed the structure of **44a** (Fig. 3a). This reaction is robust and proceeded on a 1.0 mmol scale to give **44a** in 59% yield following isolation.

We then altered the imidate substrate by changing the substituent on both the nitrogen atom and alkyne terminus in **41** (Fig. 3a). Electron-neutral (**41a**), -rich (**41b**), and -deficient (**41c**) aryl substitutions were all well tolerated. Imidates with primary (Me, **41d**) and secondary (Cy, **41e**) alkyl substitution on the nitrogen atom were also suitable. However, a bulkier *t*-butyl group on the nitrogen significantly diminished reactivity (no reaction at 150 °C), consistent with the importance of the need for initial attack by the imidate nitrogen on the DMAD partner. A *p*-iodophenyl group (**41d**) on the alkyne side didn't interfere, nor did the electron-deficient *p*-cyanophenyl group (**41f**). Beyond

aryl substitution, imidates with carboalkoxy (**41g**) and alkynyl (**41h**) on the alkyne terminus were also competent substates. The reaction also proceeds with the smaller TBS replacing the TIPS group in the amide **41a** and gave **44a'**, isolated in 63% yield on a 1 g scale reaction. Also, the bis-amide **46** (Fig. 3b) was smoothly converted to the bis-pyrrolone **47** in 70% yield after the series of: bis-silylation, bis-carbene generation, and bis-TIPS migration events.

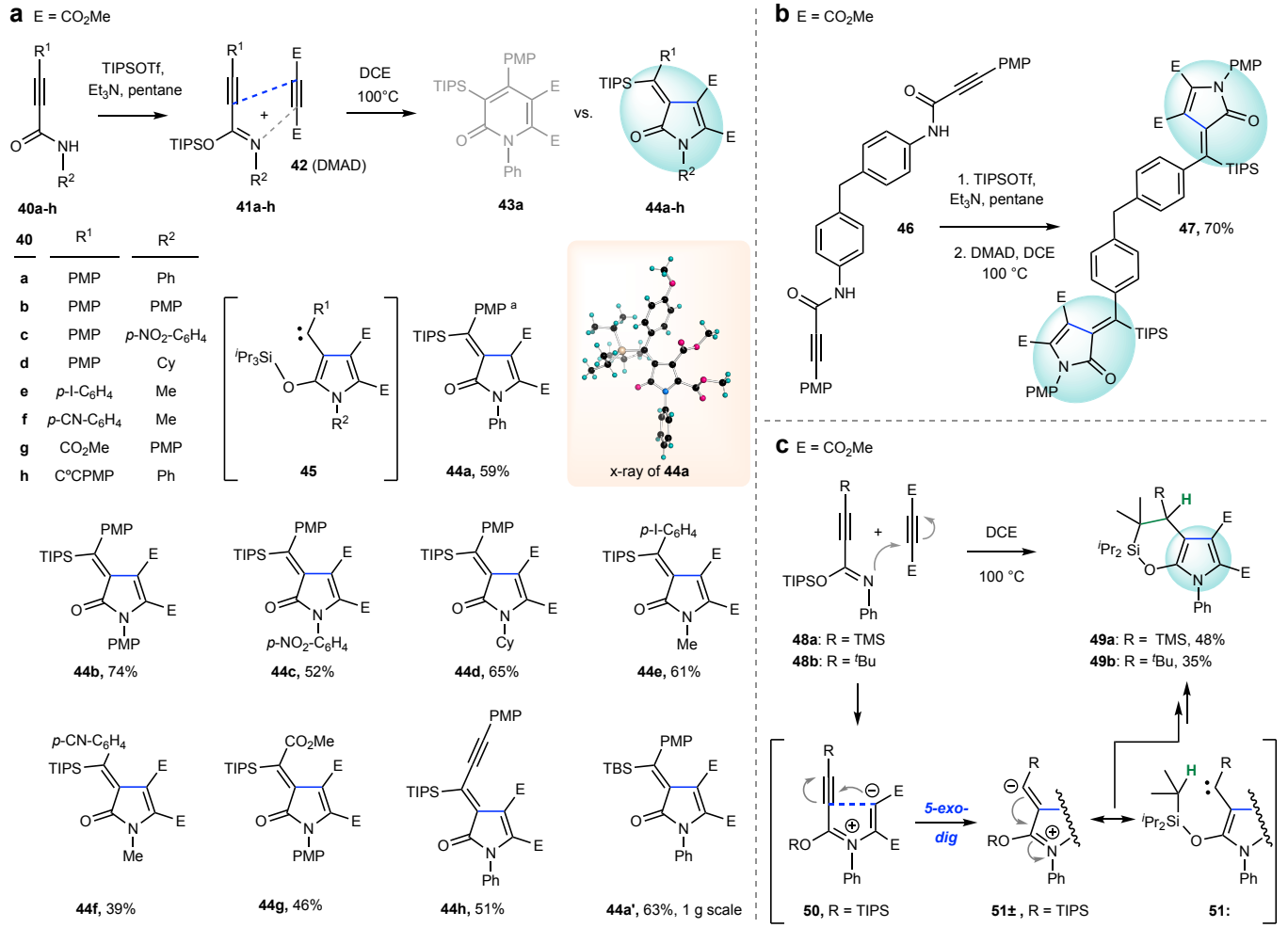

Fig. 3 | The nature of the terminal group on the alkyne of the imidate dictates the reaction pathway. a, An unsaturated substituent on the alkyne terminus leads to pyrrolone formation (**41** to **44)** via 1,4-silyl migration. **b,** Two for the price of one (**46** to **47**). **c,** A bulky substituent on the alkyne terminus inhibits silyl migration, allowing, instead, for C-H insertion by the carbene (**48** to **49**). TIPS = tri-isopropylsilyl; Tf = trifluoromethylsulfonyl; DCE = 1,2-dichloroethane; PMP = *p*-methoxyphenyl; Cy = cyclohexyl; DMAD = dimethyl acetylenedicarboxylate; TBS = *tert*-butyldimethylsilyl.

We next explored the impact of a saturated substituent on the alkynyl imidate. Although an *n*-butyl- or *iso*-propyl-alkynyl imidate was fully consumed when heated in the presence of DMAD, a very complicated product mixture was produced (crude ^{1}H NMR). When a substituent lacking a propargylic hydrogen such as TMS (**48a**, Fig. 3c) or *tert*-butyl (**48b)** was present at the alkyne terminus, clean conversion to a distinct product was observed. However, instead of pyrrolone formation (cf. **44**), the bicyclic pyrrole **49a** or **49b** was produced. This can be rationalized by a mechanistic pathway that diverges after formation of the carbene intermediate **51** via *5-exo-dig* cyclization within the zwitterion **50**. Now, due to the escalated repulsion between the bulky TMS or ^{t}Bu and silyl groups, the TIPS migration (cf. **45 to 44**, Fig 3b) was slowed, allowing time for C-H insertion to afford the pyrrole **49** as the only detected product.

After establishing the impact of the nature of the substituent on the terminus of the imidate alkyne, we turned to the use of an array of *unsymmetrical* electrophilic alkynes (**53a–f**, Fig. 4a). Reaction between each of these with the imidate derived from the amide **41b** or **52** proceeded with exclusive regioselectivity: the β-carbon of the (more) electron deficient carbonyl group was always superior (including for the case of the sulfone ester **53d**[30]) in directing the initial conjugate addition, leading to **54a–f**. We also examined the reaction between **41b** with the electron deficient allene **55** (Fig. 4b)[31]. This gave rise to **57** as a single product with defined geometry of both exocyclic alkene motifs. Notably, the lack of aromaticity within the intermediate **56** did not preclude carbene formation. Intrigued by the possibility of migration of a stannyl group, we replaced TIPSOTf with Bu_3SnOTf (Fig. 4c) to produce the stannyl imidate. The stannyl-migrated pyrrolones **59** and **60** were cleanly produced from the amides **52** and **58**, respectively. A subsequent cross-coupling reaction between the stannane **59** and 2-iodobenzothiozole (**61**) efficiently afforded the bis-heterocyclic product **62**.

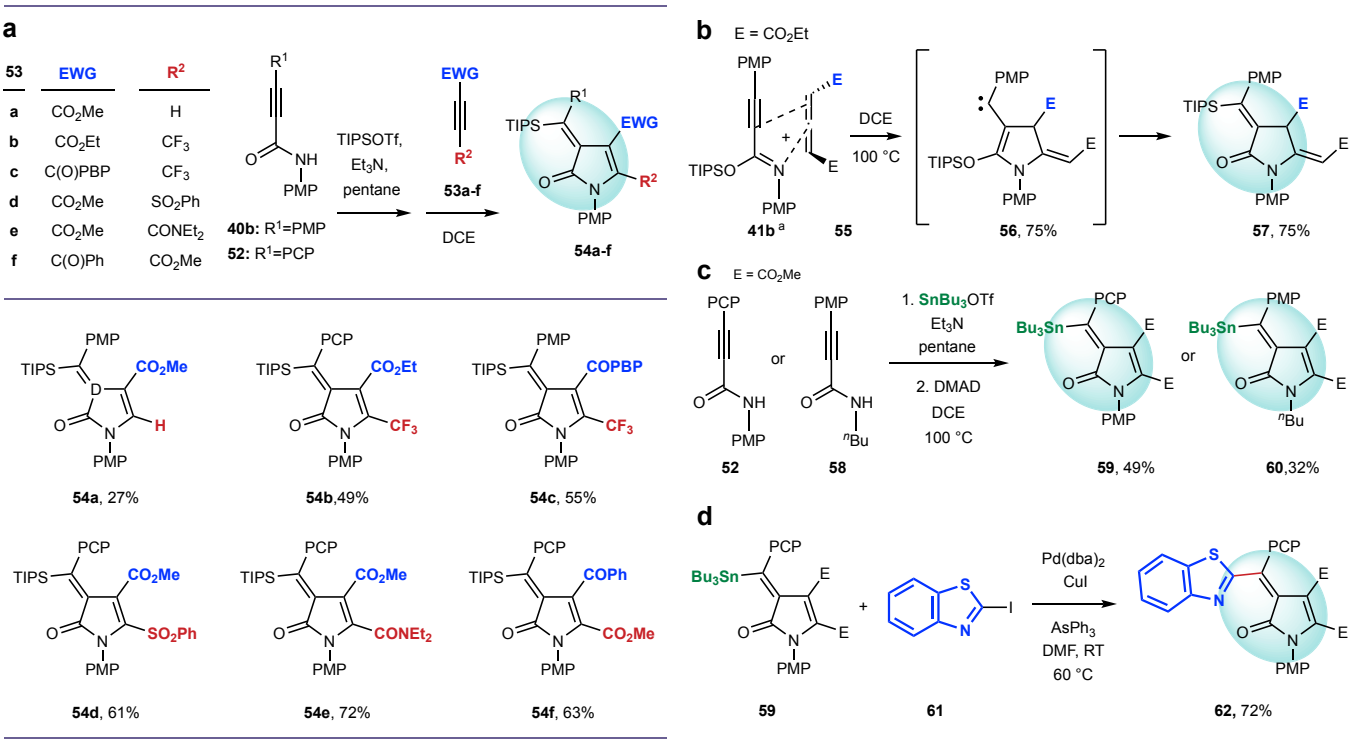

Fig. 4 | Variation of the electrophilic partners and of the migrating group. a, Unsymmetrical electrophilic alkynes participate in the (3+2) reaction with predictable and exclusive regioselectivity. **b**, Electrophilic allene **55** is a competent substrate. **c**, A Bu_3Sn group can also migrate. **d**, Cross-coupling converts the stannyl-bearing pyrrolone **59** to the bis-heterocyclic product **62**. PBP = *p*-bromophenyl; PCP = *p*-chlorophenyl; dba = dibenzylideneacetone; DMF = dimethylformamide.

[a] **41b** was formed in situ from **40b**.

With the goal of producing pyrrole derivatives rather than pyrrolones as the final products, we explored the use of simple alkynyl aldimines rather than silyl alkynyl imidates as the nucleophile that would initially engage the electrophilic alkyne (cf. **63**+**64** to **65**, Fig. 5a). Not only did this work, but the intermediate pyrrole-stabilized carbenes **65** were seen to undergo an assortment of interesting transformations. First, we treated the aldimine **66** with DMAD (Fig. 5b), which afforded the pyrrole **67** containing a dihydrobenzofuran moiety via carbene formation and a 1,5-C–H insertion reaction. Reaction of **53b** with the allyl ether **68** led to the C–H insertion products **69**; no cyclopropane formation was observed. The electrophilic alkyne partners were not limited to shelf-stable alkynes. The transient benzyne intermediate **71** derived from the triyne **70** efficiently engaged the aldimine **66** and produced the polycyclic indole derivative **72** (Fig. 5c). The reaction between **66** and the ynone **53f** led to not only the 1:1 C–H insertion adduct **73** but also the 1,3-dipolar cycloadducts **74** and **75** (Fig. 5d)[17]. Interception of the carbene carbon in **76** by the

ketone C=O oxygen atom resulted in formation of the 1,3-dipole **77**, which then was captured by a second molecule of **53f**.

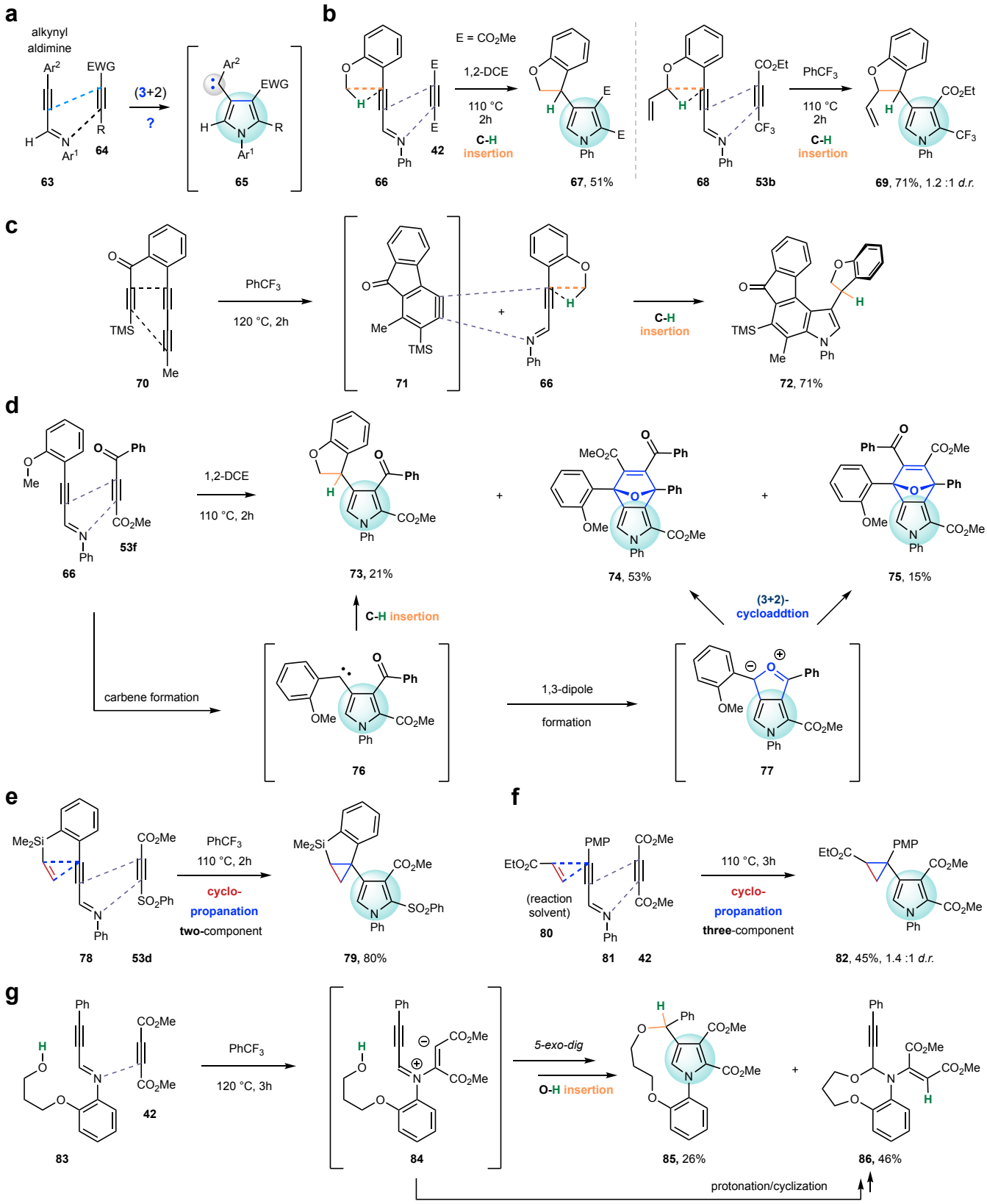

Fig. 5 | Pyrrole products from diverse types of carbene capture reactions. a, Generic formation of pyrrole-stabilized carbenes. **b**, **c**, C-H insertion using a shelf-stable alkyne or a HDDA benzyne. **d**, Competitive insertion and 1,3-dipole formation events. **e**, Intramolecular cyclopropanation. **f**, Intermolecular cyclopropanation. **g**, Macrocyclization via remote O–H insertion. d.r. = diastereomeric ratio; HDDA = hexadehydro-Diels-Alder.

Next, we examined the viability of cyclopropanation from this type of carbene. Efficient net cycloaddition reaction between the imine **78** and the alkyne **53d** and subsequent intramolecular cyclopropanation smoothy produced the pyrrole derivative **79** (Fig. 5e)[30]. The carbene from aldimine **81** and DMAD was able to engage ethyl acrylate (**80**, solvent) intermolecularly, thereby delivering the adduct **82** (Fig. 5f). It is notable that, in contrast to the electron-deficient alkene **80**, no cyclopropane product was detected when cyclohexene was instead used as the solvent, likely a reflection of the electron-rich character of the pyrrole-stabilized free carbenes **65**.

Lastly, the alkynyl aldimine **83,** containing a remotely tethered hydroxyl group was prepared and reacted with DMAD. Gratifyingly, the zwitterion intermediate **84** could undergo, albeit competitively, a *5-exo-dig* cyclization and O–H insertion to afford the macrocyclic ether **85** having 1,3-ansa bridge across the pyrrole ring. In addition, proton transfer and further cyclization within the intermediate **84** produced the 9-membered aminal **86** as a side product[32]. This result provides additional evidence for the stepwise nature of the net (3+2) cyclization; i.e., it suggests that the zwitterion **84** has a lifetime[33]. This inaugural macrocycle formation via carbene trapping is an enticing hit deserving of future exploration based on the strategic framework described here[34].

Conclusion

This study commenced with our interest in exploring whether (and how) acyclic alkynyl-substituted C=N moieties would engage electrophilic alkynes. The imino moiety took the form of either an *O*-silylimidate (cf. **41**, Fig 4a) or a simple aldimine (cf. **63**, Fig 5a). Both classes were shown to participate in a net (3+2) cycloaddition leading to five-membered ring-formation via intermediate pyrrole-stabilized free carbenes. The *O*-silylimidate precursors were formed in situ by thermal isomerization of *N*-silylamides; DFT studies were valuable in understanding both kinetic and thermodynamic aspects of this silyl tautomerization, which appears to be a facile, unimolecular event (Fig 2a). Despite the low population of the *O*-silylimidate in the quickly equilibrating mixture of silyl-tautomers, we observed conjugate addition to the electrophilic alkyne exclusively initiated by the N-atom in the imidate and a subsequent *5-exo-dig* cyclization that produced the pyrrole-stabilized carbene intermediate. DFT and NMR DP4+ analyses were instructive in differentiating carbene formation via *5-exo-dig* cyclization from a potentially competing *6-endo-dig* cyclization as the preferred pathway. These carbenes underwent retro-[1,4]-Brook rearrangement when the alkynyl imidate bore an unsaturated substituent (aryl, alkynyl, carbonyl, Fig 3a) to produce 2-pyrrolone derivatives as the product. Alternatively, a bulky substituent on the alkyne terminus (*t*-Bu or TMS) diverted the reaction pathway from silyl migration to 1,6-C–H insertion, thus delivering a bicyclic pyrrole skeleton in the product (Fig 3c). Unsymmetrical electrophilic alkynes not only participated in the cascade reaction efficiently but also showed excellent regioselectivity in the (3+2) cyclization (Fig 4a). An electron-deficient allene (**55**, Fig 4b) was also a competent electrophile. Notably, a stannyl group ($SnBu_3$) underwent analogous retro-Brook rearrangement within the pyrrole-stabilized carbene intermediate (Fig 4c); a cross-coupling reaction of the stannane product **59** provided the bi-heteroaryl product **62**. Pyrrole-stabilized carbenes derived from alkynyl aldimines also demonstrated diverse reactivity, including C–H insertion, tandem 1,3-dipole formation/(3+2) cycloaddition, cyclopropanation (intra- and intermolecular), and a notable macrocyclization (Fig. 5). In conclusion, we have discovered a fully atom-economic and catalyst- and additive-free method to produce pyrrole-stabilized carbene intermediates. The inherently high reactivity of the free carbene led to products with robustly functionalized pyrrolone and pyrrole cores.

Methods & Protocols

General procedure for the synthesis of 2-pyrrolone derivatives

The propiolamide **40** (0.1 mmol) was suspended (sometimes dissolved) in 2.5 mL of dry pentane in a 6-dram vial. Triethylamine (2.0 equiv) and the silyl triflate (1.2 equiv) were sequentially added. The reaction mixture was vigorously stirred until all of the solid material disappeared at room temperature (for soluble propiolamides, the mixture was stirred for ca. 30 min; for the less soluble propiolamides, 0.5 mL of dichloromethane was added as the co-solvent). The organic layer was carefully decanted from the precipitated Et_3N•HOTf into a clean, dry vial. After evaporative removal of the solvent, the residue was dissolved into 1 mL of, typically, 1,2-dichloroethane followed by addition of 5 equiv of DMAD. The reaction vessel was purged with N_2 and heated at the designated temperature for, typically, 20 hours. After completion of the reaction, the solvent was removed under vacuum, the residue was passed through a short column of silica (the eluting solvent is identical as the solvent for further purification), concentrated under vacuum, and purified by MPLC to give the pyrrolone products **44**.

Data availability A PDF of Supplementary Information that includes preparation procedures and characterization data for each new compound, computational methodology and results, and static copies of NMR spectra of all new compounds. Supplementary Data files: 1. Excel data sheets for NMR computations; 2. Gaussian .out files of computed geometries for conformers used in the NMR computations; 3. Cif and checkcif files for the x-ray structure of **44a**. The x-ray diffraction structure of **44a** can be found at the Cambridge Crystallographic Data Centre as Deposition Number 2431543. This data, available free of charge, can be accessed at https://www.ccdc.cam.ac.uk/structures/. A master .mnova file containing the raw data files of NMR spectra for all new compounds has been deposited in figshare[35] (DOI: 10.6084/m9.figshare.29649548).

Acknowledgements This research was enabled by a grant from the United States National Science Foundation (CHE-2155042) (T. R. H.). HRMS data (ESI) were obtained in the Analytical Biochemistry Shared Resource Laboratory of the University of Minnesota (UMN). DFT computations were performed utilizing resources provided by the UMN Supercomputing Institute (MSI). The x-ray diffraction analysis of **44a** was performed by Alex Lovstedt in the X-Ray Crystallographic Laboratory in the Department of Chemistry at the UMN.

Author contributions Q. X. performed the experimental and computational studies shown in Figs. 1-4; J. S. performed the experimental studies shown in Fig. 5. Q. X., J. S. and T. R. H. interactively interpreted the data and co-wrote the manuscript.

Competing interests The authors have no competing interests to declare.

Author Information Corresponding Author: Thomas R. Hoye − *Department of Chemistry, University of Minnesota, Minneapolis, Minnesota 55455, United States;* orcid.org/0000-0001-9318-1477; Email: hoye@umn.edu. Authors: Qian Xu − *Department of Chemistry, University of Minnesota, Minneapolis, Minnesota 55455, United States;* orcid.org/0000-0002-8655-8683. Jingyang Shi − *Department of Chemistry, University of Minnesota, Minneapolis, Minnesota 55455, United States;* orcid.org/0009-0005-7661-5380.

Figure Captions

Fig. 1 | Pyrrole is a prized heterocycle. a, Examples of pyrrole- and 2-pyrrolone-containing bioactive molecules. **b**, Examples of modern methods for synthesis of pyrroles using alkyne(s) as a building block(s). **c**. 2-Alkynyl pyridines and electrophilic alkynes fuel the formation of free carbenes conjugated to an indolizine core[17]. **d**, Tetradehydro-Diels-Alder (TDDA) reaction of **18** gives rise to the strained cyclic allene **19**. **e**, This work: two plausible competing cycloaddition pathways [(**3**+2) vs. (**4**+2)] for the reaction of **22** with **23** leading to either carbene **24** enroute to pyrrole **25** or aza-cyclic allene **26** enroute to pyridone **27**. DMA = dimethylacetamide; LCuH = liganded copper hydride; EWG = electron-withdrawing group.

Fig. 2 | DFT-computed PES for the reaction starting with 28 and 30. a, The amide tautomer **28** interconverts with its less stable imidate isomer **29** via a low-barrier unimolecular process (**TS-1**, 21.8 kcal mol^{-1}). **b**, The (3+2) cycloaddition between **29** and **30** (**TS-3**) is kinetically more favorable than the (4+2) or (2+2) pathways (via **TS-4** or **TS-5**). **c**, 1,4-Silyl migration from the oxygen to the carbon atom in carbene **32-conf-2** is the kinetically most favorable process, while the interconversion of **32-conf-1** to the allene **34** via the cyclopropene **39** has a prohibitively high barrier. TMS = trimethylsilyl; RT = room temperature;

DFT: [SMD (DCE)/B3LYP-GD3BJ/6-311++G(d,p)]. [a] The energies in Fig. 2c are all normalized to 0.0 for **32-conf-1** to more easily discern the relative energy of each stationary state in this panel. [b] Bond orders were obtained using the Wiberg bond index analysis[36].

Fig. 3 | The nature of the terminal group on the alkyne of the imidate dictates the reaction pathway. a, An unsaturated substituent on the alkyne terminus leads to pyrrolone formation (**41** to **44)** via 1,4-silyl migration. **b,** Two for the price of one (**46** to **47**). **c,** A bulky substituent on the alkyne terminus inhibits silyl migration, allowing, instead, for C-H insertion by the carbene (**48** to **49**). TIPS = tri-isopropylsilyl; Tf = trifluoromethylsulfonyl; DCE = 1,2-dichloroethane; PMP = *p*-methoxyphenyl; Cy = cyclohexyl; DMAD = dimethyl acetylenedicarboxylate; TBS = *tert*-butyldimethylsilyl.

Fig. 4 | Variation of the electrophilic partners and of the migrating group. a, Unsymmetrical electrophilic alkynes participate in the (3+2) reaction with predictable and exclusive regioselectivity. **b**, Electrophilic allene **55** is a competent substrate. **c**, A Bu_3Sn group can also migrate. **d**, Cross-coupling converts the stannyl-bearing pyrrolone **59** to the bis-heterocyclic product **62**. PBP = *p*-bromophenyl; PCP = *p*-chlorophenyl; dba = dibenzylideneacetone; DMF = dimethylformamide.

[a] **41b** was formed in situ from **40b**.

Fig. 5 | Pyrrole products from diverse types of carbene capture reactions. a, Generic formation of pyrrole-stabilized carbenes. **b**, **c**, C-H insertion using a shelf-stable alkyne or a HDDA benzyne. **d**, Competitive insertion and 1,3-dipole formation events. **e**, Intramolecular cyclopropanation. **f**, Intermolecular cyclopropanation. **g**, Macrocyclization via remote O–H insertion. d.r. = diastereomeric ratio; HDDA = hexadehydro-Diels-Alder.

References

[1] Bhardwaj, V., Gumber, D., Abbot, V., Dhiman, S. & Sharma, P. Pyrrole: A resourceful small molecule in key medicinal hetero-aromatics. *RSC Adv.* **5**, 15233–15266 (2015).

[2] Petri, G. L. *et al.* Bioactive pyrrole-based compounds with target selectivity. *Eur. J. Med. Chem.* **208**, 112783 (2020).

[3] Jeelan Basha, N., Basavarajaiah, S. M. & Shyamsunder, K. Therapeutic potential of pyrrole and pyrrolidine analogs: An update. *Mol. Divers.* **26**, 2915–2937 (2022).

[4] Singh, N. *et al.* Recent progress in the total synthesis of pyrrole-containing natural products (2011–2020). *Org. Chem. Front.* **8**, 5550–5573 (2021).

[5] Forte, B. *et al.* A submarine journey: The pyrrole-imidazole alkaloids. *Mar. Drugs* **7**, 705–753 (2009).

[6] Yen, Y.-S. *et al.* Pyrrole-based organic dyes for dye-sensitized solar cells. *J. Phys. Chem. C* **112**, 12557–12567 (2008).

[7] Pang, A. L., Arsad, A. & Ahmadipour, M. Synthesis and factor affecting on the conductivity of polypyrrole: A short review. *Polym. Adv. Technol.* **32**, 1428–1454 (2021).

[8] Guo, J.-L., Feng, Z.-M., Yang, Y.-J., Zhang, Z.-W. & Zhang, P.-C. Pollenopyrroside A and B, novel pyrrole ketohexoside derivatives from bee-collected *Brassica campestris* pollen. *Chem. Pharm. Bull.* **58**, 983–985 (2010).

[9] Tong, X.-G. *et al.* Acortatarins A and B, two novel antioxidative spiroalkaloids with a naturally unusual morpholine motif from *Acorus tatarinowii*. *Org. Lett.* **12**, 1844–1847 (2010).

[10] Shuda, M. *et al.* CDK1 substitutes for mTOR kinase to activate mitotic cap-dependent protein translation. *Proc. Natl. Acad. Sci. U.S. A.* **112**, 5875–5882 (2015).

[11] Khajuria, R., Dham, S. & Kapoor, K. K. Active methylenes in the synthesis of a pyrrole motif: An imperative structural unit of pharmaceuticals, natural products and optoelectronic materials. *RSC Adv.* **6**, 37039–37066 (2016).

[12] Philkhana, S. C., Badmus, F. O., Dos Reis, I. C. & Kartika, R. Recent advancements in pyrrole synthesis. *Synth.* **53**, 1531–1555 (2021).

[13] Estévez, V., Villacampa, M. & Menéndez, J. C. Multicomponent reactions for the synthesis of pyrroles. *Chem. Soc. Rev.* **39**, 4402–4421 (2010).

[14] Kel'in, A. V., Sromek, A. W. & Gevorgyan, V. A novel Cu-assisted cycloisomerization of alkynyl imines: Efficient synthesis of pyrroles and pyrrole-containing heterocycles. *J. Am. Chem. Soc.* **123**, 2074–2075 (2001).

[15] Gilbert, Z. W., Hue, R. J. & Tonks, I. A. Catalytic formal [2+2+1] synthesis of pyrroles from alkynes and diazenes via TiII/TiIV redox catalysis. *Nat. Chem.* **8**, 63–68 (2016).

[16] Zhou, Y., Zhou, L., Jesikiewicz, L. T., Liu, P. & Buchwald, S. L. Synthesis of pyrroles through the CuH-catalyzed coupling of enynes and nitriles. *J. Am. Chem. Soc.* **142**, 9908–9914 (2020).

[17] Xu, Q. & Hoye, T. R. Free carbenes from complementarily paired alkynes. *Nat. Chem.* **16**, 1083–1092 (2024).

[18] Guzman, A. L., Mann, A. N. & Hoye, T. R. Alkynes to (free) carbenes to polycyclic cyclopropanes. *J. Am. Chem. Soc.* **146**, 28642–28647 (2024).

[19] Xu, Q. & Hoye, T. R. A distinct mode of strain-driven cyclic allene reactivity: Group migration to the central allene carbon atom. *J. Am. Chem. Soc.* **145**, 9867–9875 (2023).

[20] Xu, Q. & Hoye, T. R. A cascade of strain-driven events converting benzynes to alkynylbenzocyclobutenes to 1,3-dien-5-ynes to cyclic allenes to benzocyclohexadienones. *J. Am. Chem. Soc.* **146**, 6438–6443 (2024).

[21] Klebe, J. F. Silyl-proton exchange reactions. *Acc. Chem. Res.* **3**, 299–305 (1970).

[22] Kashutina, M. V., Ioffe, S. L. & Tartakovskii, V. A. Silylation of organic compounds. *Russ. Chem. Rev* **44**, 733–747 (1975).

[23] Deleris, G., Dunogues, J. & Calas, R. Synthese regioselective de nitriles par voie organosilicique. *J. Organomet. Chem.* **116**, C45–C48 (1976).

[24] Wiberg, K. B. Application of the pople-santry-segal CNDO method to the cyclopropylcarbinyl and cyclobutyl cation and to bicyclobutane. *Tetrahedron* **24**, 1083–1096 (1968).

[25] Seeman, J. I. The Curtin-Hammett principle and the Winstein-Holness equation: New definition and recent extensions to classical concepts. *J. Chem. Educ.* **63**, 42–48 (1986).

[26] Kanzian, T., Nigst, T. A., Maier, A., Pichl, S. & Mayr, H. Nucleophilic reactivities of primary and secondary amines in acetonitrile. *Eur. J. Org. Chem.* **2009**, 6379–6385 (2009).

[27] Maji, B. & Mayr, H. Nucleophilic reactivities of Schiff bases. *Z. Naturforsch. B* **68**, 693–699 (2013).

[28] Minegishi, S., Kobayashi, S. & Mayr, H. Solvent nucleophilicity. *J. Am. Chem. Soc.* **126**, 5174–5181 (2004).

[29] Zanardi, M. M. & Sarotti, A. M. Sensitivity analysis of DP4+ with the probability distribution terms: development of a universal and customizable method. *J. Org. Chem.* **86**, 8544–8548 (2021).

[30] Shen, M. & Schultz, A. G. Preparation and Diels-Alder reactivity of ethyl-β-phenylsulfonylpropiolate. *Terahedron Lett.* **22**, 3347–3350 (1981).

[31] Wang, R., Xu, Q. & Hoye, T. R. Reactions of electrophilic allenoates [and isocyanates/isothiocyanates] with a 2-alkynylpyridine via a free carbene intermediate. *Org. Lett.* **26**, 7805−7808 (2024).

[32] Watson, W. On byproducts and side products. *Org. Process Res. Dev.* **16**, 1877–1877 (2012).

[33] David, O., Vanucci-Bacque, C., Fargeau-Bellassoued, M.-C. & Lhommet, G. New access to chiral cyclic ω-oxygenated β-enamino esters by intramolecular aminocyclisation reactions. *Heterocycles* **62**, 839–846 (2004).

[34] Garcia Jimenez, D., Poongavanam, V. & Kihlberg, J. Macrocycles in drug discovery─ learning from the past for the future. *J. Med. Chem.* **66**, 5377-5396 (2023).

[35] Xu, Q., Shi, J. & Hoye, T. R. Master MNova File of all NMR Spectra for Nat Synth.zip. Figshare, DOI: 10.6084/m9.figshare.29649548 (2025).

[36] Wiberg, K. B. Application of the Pople-Santry-Segal CNDO method to the cyclopropylcarbinyl and cyclobutyl cation and to bicyclobutane. *Tetrahedron* **24**, 1083–1096 (1968).